Low-Energy Structures of $(C_6H_6)_{13}$ as Determined by Low-Temperature Monte Carlo Simulations Using Several Potential Energy Surfaces

David C. Easter*

Department of Chemistry and Biochemistry, Southwest Texas State University, San Marcos, Texas 78666

Received: November 17, 2002; In Final Form: January 22, 2003

Monte Carlo computations have been carried out using six different potential energy parameter sets in order to investigate the low-energy structure(s) of $(benzene)_{13}$. Improved energies were identified for three previously published structures, and their resulting symmetries were identified. Each of the computed structures at 0.01 K is unique; however, each possesses at least one symmetry element: a C_3 rotational axis, a center of inversion, or both (i.e., an S_6 axis). From simulations at 1 K, it is hypothesized that there are two competing structures, separated by ~0.2 kJ/mol. Composite coordinates are derived for both structures with 95% confidence limits. These results can be used in conjunction with experimental data to identify the precise low-energy structure(s) of $(benzene)_{13}$.

I. Introduction

The properties and dynamics of molecular clusters are of interest for a number of reasons. Because clusters occupy the intermediate region between two extremes, represented by the isolated molecule and the bulk solid (or liquid), they possess unique size-specific properties. Cluster properties are not only intriguing in their own right, but they can often be interpreted in the context of a size-specific evolutionary sequence in order to elucidate issues regarding the minimum population required for cluster properties to converge to their respective bulk limits. Furthermore, theoretical computations using empirical nonbonded pair potentials have predicted noncrystallographic minimum-energy cluster structures;[1,2] often, these results can be tested through appropriate experimental studies.

Benzene clusters are the prototype of molecular aromatic clusters; consequently, many general properties of aromatic clusters can be deduced from studies focusing on benzene clusters. Benzene clusters are well suited for experimental study via resonance-enhanced two-photon ionization (R2PI) spectroscopy. Because the C_6H_6 molecule's first excited electronic state has an energy only slightly larger than half of the molecule's ionization potential, one-color spectra of the larger clusters can be measured without excessive interference from fragmentation effects, and two-color spectra of the larger clusters are nearly fragmentation free.[3] (For the smaller benzene clusters, however, fragmentation is an issue that must be addressed, even in two-color spectra.[4])

Ultraviolet R2PI spectral data have been interpreted in the context of the weak-interaction model in order to deduce structures of the benzene trimer and tetramer.[5−7] The model is based on the assumption that the exciton energies within the cluster are small relative to the site-energy shifts associated with each of the constituent molecules. This weak-interaction approach has been adapted to naphthalene cluster work.[8] The success of these investigations provides an optimistic outlook for determining structures of larger benzene clusters, particularly for sizes such as $N = 13$, where the structural symmetry is presumed to be high.

Several computational studies of benzene cluster structures have appeared in the literature to date. The first set of $(C_6H_6)_N$ structures, $N \in \{2,3,5,7,9,11,15\}$, was published by Williams, based on exp-6−1 nonbonded potential energy parameters.[9] This work was followed soon thereafter by that of van de Waal, in which the 13-molecule ground-state structures of several neat cluster systems, including benzene, were investigated using 12−6−1 potential functions.[10] van de Waal complemented this work with a follow-up study of smaller $(C_6H_6)_N$ structures, $N = 2-7$, this time using exp-6−1 parameters.[11] More recently, Dulles and Bartell computed structures for $N = 12-14$ using a 12−10−6−2−0 potential energy parameter set.[12] The $(C_6H_6)_{13}$ structures of Williams and van de Waal are similar in that they both have an approximate C_3 axis; however, specific points of comparison between the two structures are not included in van de Waal's report. Bartell's structure is characterized as agreeing with the other two in gross structure, but it is reported to have different molecular orientations and lower overall symmetry.[12]

On the experimental side, Easter and Whetten presented a series of reports on benzene clusters, based on both 1- and 2-color R2PI ultraviolet spectroscopy.[3,13] A paradox arising from those reports is noteworthy. On one hand, the absence of a spectral feature corresponding to the $B_{2u} \leftarrow A_{1g}$ 0_0^0 transition of the central molecule (present in the corresponding 6_0^1 spectrum) provides support for a cluster structure with C_3 (or higher) symmetry.[3] On the other hand, a doublet is observed in the corresponding spectral feature of the 6_0^1 spectrum for the isotopically substituted $(C_6H_6)(C_6D_6)_{12}$ cluster, implying a symmetry lower than C_3.[13] This apparent discrepancy is echoed by the differences in reported symmetries of the computed $(C_6H_6)_{13}$ structures, summarized in the previous paragraph.

To investigate this question, we have carried out Monte Carlo simulations of $(C_6H_6)_{13}$ structures using six different potential energy parameter sets (including those that were used by Williams, van de Waal, and Bartell). Each of our computations was conducted within a common coordinate system, allowing for a direct comparison between the resulting structures. Although the computed ground-state structures are each unique, they share more in common than might be inferred from the original reports. Concurrent analysis of all of the structures

* To whom correspondence should be addressed. E-mail: Easter@swt.edu.

10.1021/jp027475s CCC: $25.00
Published on Web 03/13/2003

makes it possible to establish structural (coordinate) *boundaries* within which the true structure(s) should exist. It is intended that these results will, when combined with spectroscopic data and a weak-interaction model, make it possible to accurately deduce the optimal $(C_6H_6)_{13}$ structure(s).

II. Potential Energy Surfaces

Six different nonbonded pair potential energy functions were used in our simulations. We describe each of them here. Originally published parameter values are not duplicated in this report, and the reader is referred to the original literature to obtain those values. However, a *unified* parameter scheme is presented in the Appendix of this paper, and parameter values (within the unified scheme) are tabulated for each of the six potential energy surfaces.

A. Williams. The first parameter set employs the *exp-6−1* potential energy function of Williams and Starr, which has the form, $V_{jk} = B\exp(-Cr_{jk}) - Ar_{jk}^{-6} + q_jq_kr_{jk}^{-1}$.[14] In this function, A, B, and C represent potential energy parameters that depend on the identities of interacting atoms (j and k), r_{jk} is the separation between atoms, and q_j represents the partial atomic charge of atom j. The fixed molecular bond distances are assumed to be 1.397 and 1.027 Å for C−C and C−H, respectively.

This was the parameter set used by Williams in his determination of benzene cluster structures;[9] it has subsequently been adapted to other functional forms, two of which were utilized in this study.[10,15] (We subsequently refer to this set as the Williams parameters). In general, the Williams parameters have been found to reproduce a broad range of experimental data; in addition, the general framework can be transferred to compounds other than benzene.[15] One precaution must be observed when using the Williams parameters at higher temperatures and larger step sizes. The functional form is such that the attractive (r^{-6}) term dominates the sum when the value of r is very small. Therefore, to avoid potential (nonphysical) complications in simulations with larger step sizes, we identified the value of r corresponding to the *maximum* of each potential function. The resulting distances, 0.786, 0.853, and 0.927 Å, for the C−C, C−H, and H−H interactions were set as the *minimum* distances required to "switch on" the r^{-6} term in each sum.

B. van de Waal. The second parameter set, used in van de Waal's study of several 13-molecule cluster structures, is based on a Lennard-Jones function, with a Coulombic term added. The function has the form

$$V_{ij}(r) = 4\epsilon_{ij}\left[\left(\frac{\sigma_{ij}}{r}\right)^{12} - \left(\frac{\sigma_{ij}}{r}\right)^{6}\right] + C\frac{q_iq_j}{r}$$

where ϵ_{ij} and σ_{ij} represent Lennard-Jones parameters, and C is a conversion factor that yields units of kJ mol^{-1} when r is expressed in Å, and q has units of e.[10] (The magnitude of the potential energy parameter corresponding to the r^{-1} term is given by the product Cq^2.) van de Waal derived the 12−6−1 parameter set from the Williams parameters by fitting both the positions and the depths of the respective Lennard-Jones curves; his motivation was to make computation more rapid. In his report, van de Waal tabulated two distinct sets of parameter values for carbon−carbon interactions: one specific to hydrocarbons and the other specific to carbon dioxide. van de Waal used the *hydrocarbon*-specific values in his benzene cluster work. (We subsequently refer to this parameter set as the van de Waal parameters.)

Like Williams, van de Waal assigns a partial charge of +0.153 e to each hydrogen atom and then quotes a value of 1389.963 kJ Å mol^{-1} e^{-2} for the conversion factor, C. The conversion factor is given by the relationship

$$C = \left(\frac{F_{\mathrm{mA}}}{4\pi\epsilon_{\mathrm{o}}}\right)(F_{\mathrm{eC}})^2N_{\mathrm{A}}(F_{\mathrm{kJ}})$$

where ϵ_{o} is the permittivity of vacuum, N_{A} is Avogadro's number, and F_{mA}, F_{eC}, and F_{kJ} each represent unit conversion factors: m → Å; e → C; and J → kJ. Using currently accepted values for the physical constants and conversion factors, we calculate a slightly *smaller* value for C, 1389.376.[16] With q = 0.153 e, $C(q^2/°A)$= 32.523 kJ/mol using our constant; the value resulting from van de Waal's value is 32.538 kJ/mol. Although the difference is not large, it is sufficient to make a difference of 0.03 kJ/mol (0.009%) in the energy of our optimized $(benzene)_{13}$ structure. In this work, we have used the more recent (1998) values for the physical constants. Molecular bond distances assumed by van de Waal were 1.397 and 1.027 Å, after Williams.

C. Shi(5). The third parameter set, used in the study of Dulles and Bartell, is based on the functional form, $V_{jk} = Ar_{jk}^{-12} + Br_{jk}^{-10} + Cr_{jk}^{-6} + Dr_{jk}^{-2} + K$.[12] Parameters for the 12−10−6−2−0 potential were derived by Shi and Bartell from the parameters of Karlström but were rescaled and simplified (eliminating all odd powers of 1/r) to facilitate rapid computation.[17] In his original parameter set, Shi imposed a 5-Å cutoff for the parametrized quasi-electrostatic term, $Dr_{jk}^{-2} + K$; Dulles subsequently made modifications, extending the cutoff to 12 Å.[12] As Dulles comments, care must be exercised when calculating hydrogen−hydrogen potentials when using larger step sizes, because the sign of the r^{-12} term results in nonphysical potential energies at small values of r. We have addressed this issue by determining the position of the *maximum* of the V_{HH} function (1.370 Å) and have instituted this as the minimum distance required for switching on the r^{-12} term in the V_{HH} potential.

Statistical analysis of the Dulles−Bartell atomic positions, published for $(C_6H_6)_{13}$, reveals that the molecular C−C and C−H bond lengths were *not* held constant, with average empirical bond lengths of 1.3992 ± 0.0003 Å (C−C) and 1.0284 ± 0.0002 Å (C−H).[12] These empirical averages are respectively 0.13% and 0.25% smaller than the *fixed*-distance bond lengths (1.401 and 1.031 Å) quoted by Dulles (as corrected by Niesse and Mayne[18]). In some preliminary calculations, we employed the *averaged* bond distances. Except where otherwise noted, however, final simulations made use of the *fixed* bond distances (1.401 and 1.031 Å). (We subsequently refer to this parameter set as the Shi(5) parameters.)

D. Shi(3). The fourth parameter set, also developed by Shi and Bartell, is based on a 12−6−1 functional form, $V_{jk} = Ar_{jk}^{-12} + Br_{jk}^{-6} + Cr_{jk}^{-1}$ [12] and will subsequently be referred to as the Shi(3) parameters. Although it has similarities to the van de Waal potential function, the Shi(3) function differs in that parameters for the repulsive (r^{-12}) and attractive (r^{-6}) terms are uncoupled. The value of the Coulombic parameter, C, can be used to infer a partial atomic charge of ±0.147 e, 4% smaller than the value assumed by both Williams and van de Waal (±0.153 e). Given that, like the Shi(5) parameters, the Shi(3) parameter set was developed specifically to describe systems containing benzene dimers, it was deemed appropriate for inclusion in this study. Fixed bond distances are assumed to be 1.401 and 1.031 Å.

TABLE 1: Easter(B13) Parameters[a]

12-9-6-4-1	r^{-12}	r^{-9}	r^{-6}	r^{-4}	r^{-1}
C−C	2315968	140670	−2109.14	−155.880	25.8549
C−H	329744.1	14426.6	−1857.42	147.528	−25.8549
H−H	37181.5	−5185.4	743.55	−139.175	25.8549

[a] Parameters were scaled from the Karlström 12−9−6−4−1 function to match the optimal C−H interaction distance and the best energy for $(C_6H_6)_{13}$. Resulting energy values are in kJ/mol when r is in Å.

E. Karlström. The fifth parameter set, developed by Karlström et al., the foundation from which the Shi(5) parameters were derived, utilizes a 12−9−6−4−1 functional form: $V_{jk} = Er_{jk}^{-12} + Dr_{jk}^{-9} + Cr_{jk}^{-6} + Br_{jk}^{-4} + Ar_{jk}^{-1}$.[17] (This is subsequently referred to as the Karlström parameter set.) Karlström parameters were derived from ab initio SCF−CI calculations specifically to account for benzene−benzene interactions; as a result, the parameter set is not generally transferable to systems containing molecules other than benzene. When used in the context of Monte Carlo simulations of bulk liquid and solid benzene, these parameters were successful in reproducing much of the bulk experimental data.[19] However, as pointed out by Shi, the application of Karlström parameters to computations involving benzene dimers results in incorrect scaling for both energies and intermolecular distances.[15] These difficulties notwithstanding, the parameter set was included in our study primarily because it is the foundation from which the Shi(5) parameters were derived. Although the resulting energies and interaction distances for $(C_6H_6)_{13}$ are incorrectly scaled, it is nevertheless reasonable to expect that information will be gained both about the molecular angular positions (Θ, Φ) and orientations. The fixed molecular bond distances are assumed to be 1.395 and 1.084 Å.

F. Easter(B13). Following completion of simulations using the first five parameter sets, we derived a sixth parameter set, subsequently referred to as the Easter(B13) parameters. We used the Karlström 12−9−6−4−1 functional form and assumed the same molecular bond distances (1.395 and 1.084 Å). Analysis of the first four parameter sets suggests an optimal C−H interaction distance of ∼2.9 Å, and a best energy for $(C_6H_6)_{13}$ near ∼325.1 kJ/mol. The Easter(B13) parameters (shown in Table 1) are the product of rescaling the Karlström parameters in order to reflect these values.

The six potential energy parameter sets are plotted together in Figure 1. Three observations are worth comment. (1) The location of the repulsive wall (short distances) differs among parameter sets. (2) The repulsive wall of the Williams (exp-6−1) parameters rises less steeply than the others. (3) The Shi(5) function approaches zero more rapidly at larger distances than do the other functions, a direct consequence of parametrizing the electrostatic term.

III. Procedure

A. Monte Carlo Computations. The computer code used for carrying out simulations within the Metropolis Monte Carlo Method[20] was developed in our laboratory. A typical simulation consists of 10^5 Monte Carlo steps per temperature cycle, with a total of 10^2 temperature cycles. Initial parameter step sizes were determined from coordinate standard deviations in preliminary simulations; the step sizes were subsequently adjusted at the beginning of each temperature cycle to ensure an acceptance rate of 50 ± 5%. Six parameters were used to define the position and orientation of each molecule: the molecule's center of mass was described by the use of spherical polar coordinates, (R, Θ, Φ); its orientation was described in terms

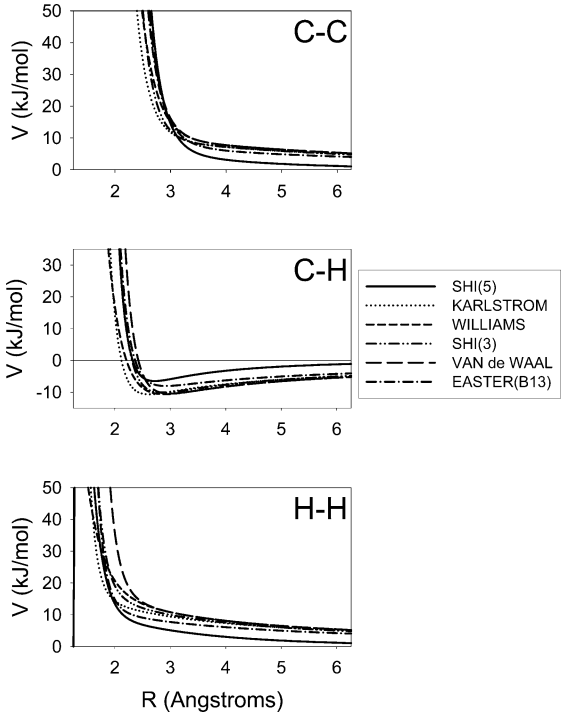

Figure 1. Nonbonded atom−atom potential energy functions used in this work. Potential energy is plotted vs distance for the C−C, C−H, and H−H nonbonded atom−atom interactions.

of Euler angles, (α, β, γ). The spherical polar coordinates are related to Cartesian coordinates through standard transformations: $x = R \sin\Theta \cos\Phi$; $y = R \sin\Theta \sin\Phi$; and $z = R \cos\Theta$. Euler rotations were applied in the following order: (1) $R_z(\alpha)$, rotation about the z axis (from the x axis toward the y axis); (2) $R_y(\beta)$, rotation about the y axis (from the z axis toward the x axis); (3) $R_z(\gamma)$, rotation about the z axis. Standard matrixes for the Euler rotations are

$$R_z(\alpha) = \begin{pmatrix} \cos\alpha & \sin\alpha & 0 \\ -\sin\alpha & \cos\alpha & 0 \\ 0 & 0 & 1 \end{pmatrix}$$

and

$$R_y(\beta) = \begin{pmatrix} \cos\beta & 0 & -\sin\beta \\ 0 & 1 & 0 \\ \sin\beta & 0 & \cos\beta \end{pmatrix}$$

The $R_z(\gamma)$ rotation is identical in form to $R_z(\alpha)$.[21]

Incorporated within the computer code was an option to run each simulation either with or without imposing specific symmetry constraints on the structure. Three options included S_6, C_3, and C_i symmetries; an additional option permitted the central molecule to break symmetry while imposing constraints on the ligand molecules. In all of the symmetry-constrained simulations, symmetry-related molecules were moved as a group. With the exception of simulations in which the central molecule was allowed to break symmetry, each move of the central molecule was compensated by a coordinate system shift; consequently, all structures are reported within the same coordinate system.

B. Coordinate System and Symmetry Operations. To facilitate the direct comparison of structures, the standardized coordinate system shown in Figure 2 was established. The three published $(C_6H_6)_{13}$ structures are consistent in that they identify a unique central molecule surrounded by a shell of twelve ligand

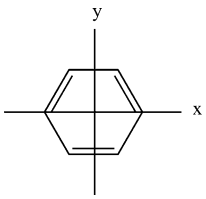

Figure 2. Standardized cluster right-handed coordinate system. The plane of the central molecule (shown) defines the cluster $x-y$ plane, with the x axis being defined by a pair of opposing C−H bonds. The z axis (not shown) is perpendicular to the molecular plane and passes through the molecule's center of mass.

TABLE 2: Symmetry Operations[a]

E	S_6	$C_3 = S_6^2$	$i = S_6^3$
R	R	R	R
Θ	$\pi - \Theta$	Θ	$\pi - \Theta$
Φ	$\Phi + \pi/3$	$\Phi + 2\pi/3$	$\Phi + \pi$
α	$\alpha + \pi$	α	$\alpha + \pi$
β	β	β	β
γ	$\gamma + 4\pi/3$	$\gamma + 2\pi/3$	γ

[a] The operations are applied to transform a set of position (R, Θ, Φ) and orientation (α, β, γ) coordinates, to the corresponding coordinates of a symmetry-related molecule. Angles (here and in subsequent tables) are in radians.

molecules. The benzene molecule has D_{6h} symmetry, thus defining all of the molecule's interatomic angles; however, the C−C and C−H bond lengths for each calculation are defined differently, depending on the specifications of each parameter set. In our right-hand coordinate system, the plane of the central molecule defines the cluster $x-y$ plane, and the line passing through the molecule's center of mass that is perpendicular to the molecular plane is the cluster z axis. The x axis is arbitrarily defined by two of the central molecule's opposing C−H bonds.

Because many of our simulations were carried out with imposed symmetry restrictions, it was necessary to move all symmetry-related molecules simultaneously. The choice of representing molecular centers by spherical polar coordinates and orientations by Euler angles was well suited for the task. Given the six coordinates for a ligand molecule, coordinates are generated for all symmetry-related molecules using the operations in Table 2. For simulations restricted to S_6 symmetry, the coordinates of only two unrelated ligand molecules are required; coordinates of the 10 remaining ligands are generated through the sequential application of the S_6 operation. For C_3-symmetry calculations, there are four independent groups of ligand molecules and six groups for C_i calculations.

Because of the C_6H_6 molecule's D_{6h} symmetry, the six carbon atoms are structurally equivalent; nevertheless, the symmetry operations in Table 2 treat each atom as *distinguishable*; as a result, each operation yields the correct result in the eventuality that a ^{13}C or ^{2}D label is selectively placed within a specific molecule. This feature of the operations will be particularly useful for future calculations in which both vectors (transition dipole moments) and tensors (quadrupole moments and polarizabilities) will be transformed based on the associated molecule's assumed structural symmetry.

Given that the three published $(C_6H_6)_{13}$ structures agree in *gross* geometry, we established a molecular numbering scheme (Figure 3) for the purpose of identifying and distinguishing each of the thirteen constituent molecules. The structure shown has S_6 symmetry (the *highest* symmetry predicted by simulations). Other symmetries (C_3 and C_i) are derived by applying perturbations to the S_6 structure. The S_6 structure consists of three symmetry-distinct sets of molecules: (1) the central molecule;

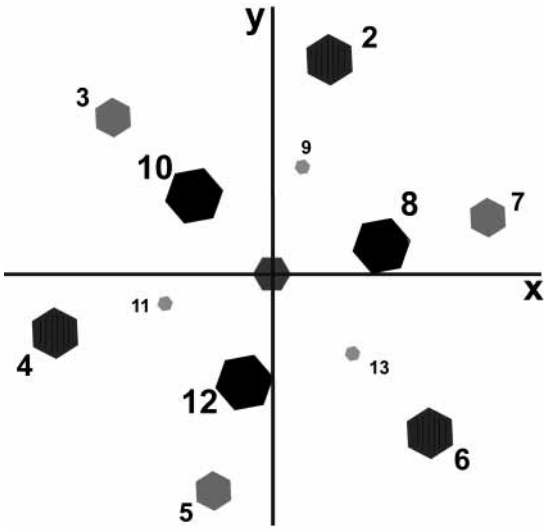

Figure 3. Simplified structure of $(benzene)_{13}$, viewed from the $+z$ axis, with the x axis defined by two of the central molecule's C−H bonds. Molecular orientations are not represented. Larger, darker hexagons represent benzene molecules with larger $+z$ coordinates; as the z coordinate decreases, the hexagon size decreases, and the shading becomes lighter. The structure shown has S_6 symmetry, containing both a C_3 rotational axis (the z axis), and a center of inversion (the origin). (For a visual comparison of C_3 and C_i structures, see Figure 8.)

(2−7) the six *equatorial* molecules surrounding the central molecule have z coordinates that alternate above/below the $x-y$ plane ($\sim\pm1$ Å); and (8−13) the six *cap* molecules form a staggered pair of equilateral triangles, located approximately ±4.5 Å above and below the $x-y$ plane. For the C_3 structure, the *upper equatorial* molecules (2, 4, 6) must be distinguished from the *lower equatorial* molecules (3, 5, 7); similarly, the *upper cap* (8, 10, 12) must be distinguished from the *lower cap* (9, 11, 13). When the signs of *all* Cartesian coordinates in a cluster structure are simultaneously changed, the energy of the *inverted* structure is identical to that of the original; consequently, to avoid ambiguity, we define the positive direction of the z axis for a C_3 structure such that the cluster's center of mass lies on the $+z$ axis. For cluster structures with only inversion (C_i) symmetry, there are six symmetry-distinct ligand groups: {2, 5}, {3, 6}, {4, 7}, {8, 11}, {9, 12}, and {10, 13}. To ensure consistency, we define the right-hand coordinate system for C_i structures such that the distance coordinates of equatorial molecules always decrease in the order, $R(2) > R(4) > R(6)$.

Two distinct starting configurations were used for initial simulations. The first of these was derived from Williams' *isotridecamer* cluster [see Section IV. A.].[9] After generating 156 atomic coordinates, new coordinates were derived to reflect the molecular positions (R, Θ, Φ) and orientations (α, β, γ). (The Euler angles were determined from nonlinear least-squares fits, after taking into account that the application of the Williams rotational matrixes frequently interchanges symmetry-equivalent atoms.) Finally, each of the constituent molecules was numbered according to Figure 3.

The second starting configuration was derived from published atomic positions of the Dulles−Bartell structure, after transformation to our molecular coordinate system.[12] Because the specific correlation between the Williams and Dulles coordinate systems was unclear, preliminary simulations were conducted using the Williams and the Shi(5) parameter sets. When simulations starting with the two initial structures yielded identical energies separately within each parameter set, a

TABLE 3: Calculated Lowest Energies for the $(C_6H_6)_{13}$ Cluster with Specified Symmetries at 0.01 K[a]

parameter set symmetry	Williams −325.308	van de Waal (−325.1)	Shi(5) −325.083	Shi(3)	Karlström	Easter(B13)
S_6	**-325.329**	−325.049	−322.507	−325.665	−371.849	
C_3	−325.329	**−325.272**	−323.068	**−326.223**	**−372.960**	−324.892
C_i	−325.329	−325.105	**−325.096**	−325.891	−372.883	**−325.116**
unrestricted	−325.329	−325.272	−325.096	−326.223	−372.960	−325.116

[a] Boldfaced entries indicate the highest-symmetry structure for which the computed energy is a global minimum. Calculated energies of *published* structures are included in the first row; van de Waal's reported energy is also shown. Here (and in subsequent tables) energies are in units of kJ/mol. The inherent error in calculating energy values is estimated to be ~±0.005 kJ/mol.

correlation between the two systems was possible. We established that the two structures could be described within a common coordinate system by (1) applying Euler rotations to the Dulles−Bartell coordinate system, (2) renumbering the ligand molecules (according to Figure 3), and then (3) renumbering each molecule's atoms in order to ensure consistency with the rotation operations (in Table 2). The resulting two structures, after transformation from the Dulles−Bartell coordinate system was completed, were identical to the structures described within the Williams coordinate system.

C. Sequence of Calculations. To verify the equivalence of our two initial configurations to those originally published, potential energies were calculated for the two static structures. Williams reported an energy of −325.3 kJ mol^{-1} for his isotridecamer cluster;[9] our energy, based on the *atomic positions* generated from his matrixes, is −325.312 kJ mol^{-1}, and the value obtained by generating atomic positions from our derived molecular coordinates (R, Θ, Φ, α, β, γ) is −325.308 kJ mol^{-1}. The difference of 0.004 kJ mol^{-1} is not significant and may be taken as a measure of the inherent error in these energy calculations.

The Dulles−Bartell structure was reported to have an energy of −324.915 kJ mol^{-1}.[12] On the basis of the *published atomic coordinates*, we calculated a cluster energy of −324.852 kJ mol^{-1}. Using our molecular coordinate system (R, Θ, Φ, α, β, γ), the corresponding energy is −324.844 kJ mol^{-1} when we used the *average* (empirical) bond distances, inferred from analysis of the atomic positions. The energy is −325.083 kJ mol^{-1} when the *fixed bond distances* quoted by Dulles are used within our molecular coordinate system. The difference between the first two values, −324.852 and −324.844 kJ mol^{-1}, arises from the variation in bond distances reflected in Dulles' original coordinates;[12] the difference between the latter two values, −325.083 and −324.844 kJ mol^{-1}, stems from differences between the *average* bond distances and the *quoted* bond distances. Why none of our calculated energies exactly matches that of Dulles (−324.915 kJ mol^{-1})[12] is not entirely clear. We only conjecture that the energy quoted by Dulles may possibly be based on a structure whose atomic coordinates differ slightly from those that were published. In all of our subsequent simulations, the *fixed* bond-distances were assumed, and an energy of −325.083 kJ mol^{-1} (our calculated value) was assigned to the Dulles−Bartell structure.

Following our preparatory work, several series of simulations were conducted. The first two sets of simulations involved cooling the clusters from 100 to 1 K by temperature steps of −1 K; no restrictions were placed on cluster symmetry in the first of these, but S_6 symmetry was imposed in the second. The lowest-energy structure thus determined for each parameter set was used for the initial configuration in subsequent simulations wherein the clusters were cooled from 1 to 0.01 K by temperature steps of −0.01 K.

Additional simulations, all involving cluster cooling from 1 to 0.01 K, separately imposed the following symmetries: C_3, C_i, S_6*, C_3*, and C_i*, with the latter three simulations permitting the *central* molecule to break symmetry, while imposing symmetry on all the ligands. Finally, the 1−0.01 K simulation was repeated with no symmetry restrictions in order to search for any ground-state configurations that might have been overlooked.

TABLE 4: Molecular Coordinates for the Ground-State Structure (0.01 K), Based on the Williams Parameter Set (E = −325.33 kJ mol^{-1})[a]

molecule	energy/ kJ mol^{-1}	R/ Å	Θ	Φ	α	β	γ
2	−22.13	5.2718	1.3675	1.3050	0.8583	1.3462	1.8161
8	−24.19	5.4488	0.5719	0.2537	0.7739	1.3004	2.5553

[a] Here (and in subsequent tables) R is given in angstroms. Individual molecular interaction energies are shown in the second column; the interaction energy of the central molecule is −47.39 kJ/mol. Coordinates of the remaining 10 ligand molecules are generated by sequential application of the S_6 symmetry operation (see Table 2).

IV. Results

Computed energies are summarized in Table 3 for each set of potential energy parameters within four specific cluster symmetries. For each parameter set, the *highest*-symmetry structure corresponding to the global energy minimum is boldfaced. Because none of the simulations that permitted the central molecule to break symmetry resulted in an energy gain, results of those simulations are not shown.

A. Structures based on the Williams Parameters. The ground-state cluster structure at 0.01 K derived from the Williams parameters has S_6 symmetry. Although Williams' description of his *isotridecamer* as having "an approximate 3-fold axis of symmetry" understates the true symmetry, the description is consistent with positions generated by his rotation matrixes.[9] Our computed structure shows an improvement in energy. Although the difference (0.021 kJ/mol) is small, it establishes the assignment of S_6 symmetry to the Williams (*isotridecamer*) structure. (The Williams *isotridecamer* is qualitatively similar in to the S_6 structure reported in Table 4 and illustrated in Figure 3; quantitatively the *isotridecamer*'s coordinates are characterized by small coordinate displacements relative to those of the S_6 structure.)

The S_6 structure contains two unique groups of ligands. Each of the six *equatorial* molecules is situated 5.272 Å from the cluster origin and is positioned ±1.064 Å from the $x-y$ plane; each has a molecular inclination of β = 77.13° (where β measures the angle included between the cluster z axis and the natural molecular z axis) and has an interaction energy of −22.13 kJ/mol. Each of the six *cap* molecules is located 5.449 Å from the origin and is positioned ±4.582 Å from the $x-y$ plane; each is inclined at 74.51° and has an interaction energy of −24.19 kJ/mol. The interaction energy of the central molecule is −47.39 kJ/mol, in agreement with the value reported by Williams (−47.4 kJ/mol).

TABLE 5: Averaged Molecular Coordinates at 1 K Using the Williams Parameters[a]

molecule	energy	R/Å	Θ	Φ	α	β	γ
2	−21.70	5.340	1.357	1.298	0.818	1.348	1.862
	(0.10)	(0.026)	(0.009)	(0.006)	(0.028)	(0.014)	(0.019)
3	−22.53	5.206	1.764	2.356	4.034	1.342	5.952
	(0.15)	(0.021)	(0.008)	(0.007)	(0.015)	(0.015)	(0.016)
8	−24.33	5.449	0.573	0.261	0.775	1.294	2.561
	(0.13)	(0.016)	(0.007)	(0.012)	(0.011)	(0.020)	(0.019)
9	−23.96	5.449	2.570	1.288	3.916	1.303	0.447
	(0.12)	(0.017)	(0.011)	(0.024)	(0.011)	(0.027)	(0.018)

[a] Within the uncertainty of the simulation, the structure has C_3 symmetry. The mean cluster energy in simulations at 1 K is −325.02 ± 0.04 kJ mol^{-1}, and the central molecule's stabilization energy is −47.4 kJ/mol. Standard deviations for each coordinate are shown in parentheses.

TABLE 6: Molecular Coordinates of the Ground-State C_3 Structure (0.01 K), Based on the Van De Waal Parameter Set (E = −325.27 kJ mol^{-1})[a]

molecule	E (0.12)	R (0.021)	Θ (0.014)	Φ (0.021)	α (0.014)	β (0.022)	γ (0.016)
2	−21.007	5.4931	1.3348	1.3004	0.7455	1.3476	1.9354
3	−23.010	5.1647	1.7530	2.3685	4.0770	1.3295	5.8944
8	−24.736	5.5132	0.5664	0.2800	0.7746	1.3080	2.5872
9	−23.796	5.5036	2.5764	1.2884	3.9126	1.3231	0.4609

[a] Molecular interaction energies are shown in the second column. Coordinates of the remaining eight ligand molecules are generated by sequential application of the C_3 symmetry operation. Average coordinates from simulations at 1 K agree with ground-state values within ±0.001; composite standard deviations (first row, parentheses) are based on 1 K simulations with unrestricted symmetry.

With the long-range motivation of correlating theoretical structures to experimental data, the ground state (S_6) structure was used as the initial configuration to compute *average* coordinate values and their standard deviations in simulations (with no symmetry restrictions) at 1 K. The resulting coordinates are collected in Table 5. Somewhat unexpectedly, the simulations reveal that the *average* cluster structure at 1 K is distinct from the ground-state structure; it has lower overall symmetry (i.e., C_3 instead of S_6). The static energy of the mean (C_3) configuration is −325.30 kJ/mol; the mean cluster energy observed in the simulations is −325.02 kJ/mol. The upper equatorial molecules, on average, are found 0.07 Å further from the nucleus, relative to their position in the ground state (with a compensating −0.07 Å shift for the lower equatorial molecules). The cap molecules remain equally distanced from the central molecule (5.449 Å), but their mean interaction energies are distinct.

B. Structures based on the van de Waal Parameters. The ground state $(C_6H_6)_{13}$ structure calculated from the van de Waal parameters has C_3 symmetry and an energy of −325.272 kJ/mol. Coordinates of four symmetry-distinct molecules (2, 3, 8, and 9) are collected in Table 6. The upper equatorial molecules are located at a distance of 5.493 Å from the cluster center, 1.284 Å from the $x-y$ plane, and are inclined at an angle of 77.21°; their lower equatorial counterparts are located at 5.165 Å from the cluster center, 0.936 Å from the $x-y$ plane, with an inclination angle of 76.17°. The upper cap molecules are located at 5.513 Å, 4.652 Å from the $x-y$ plane, with an inclination of 74.94°; the lower cap molecules are located at R = 5.504 Å, are distanced 4.648 Å from the $x-y$ plane, and have an inclination of 75.81°. The stabilization of the central molecule in this structure is −47.625 kJ/mol; stabilization energies of the four distinct ligand molecules are summarized in Table 6. In the C_3 configuration, the center of mass of the ligand molecules is located at z = +0.088 Å.

The mean cluster energy in simulations at 1 K is −325.0 kJ/mol, whereas the static energy of the *average* structure is −325.27 kJ/mol. Average coordinate values at 1 K reflect the ground-state C_3 structure. In every instance except one, the *average* coordinate value differs by no more than ±0.001 from its ground state (the exception being R(3), which differs by 0.002 Å); furthermore, average molecular stabilization energies are all within 0.1 kJ/mol of the ground state. Composite standard deviations of the average coordinates are included in the first row of Table 6.

The structure reported by van de Waal is not accompanied by data that is sufficient to reconstruct atomic positions.[10] van de Waal's structure is described as following a noncrystallographic pentagonal motif that is close to a regular icosahedron, with an energy of −325.1 kJ/mol. van de Waal does not distinguish between upper and lower equatorial molecules; these are described as being located a distance of 1.06 Å from the $x-y$ plane at a total distance of 5.27 Å from the cluster center, with an inclination angle of 77.10°. Similarly, the upper and lower cap molecules are not distinguished and are collectively described as being 4.58 Å from interior molecule's molecular plane at total distance of 5.58 Å from the cluster center, with an inclination angle of 74.50°. From van de Waal's description, an S_6 structure is inferred, based on the lack of distinction between upper and lower equatorial/cap molecules. van de Waal's values are remarkably similar to those that we have identified for the Williams S_6 structure: three of the distance coordinates cited by van de Waal agree exactly with those of the Williams structure; the longer of the two radial distances differs from Williams by 0.13 Å, and the angles of inclination differ by only 0.03° and 0.01°.

The reasons for the apparent discrepancy between our ground state structure and that described by van de Waal are difficult to pinpoint because of the absence of specific detail in van de Waal's original paper. Not only does our ground-state structure have a *lower* overall symmetry (C_3 vs S_6), it also has improved overall energy (−325.27 vs −325.1 kJ/mol). In our preliminary S_6 symmetry-constrained simulations (using van de Waal's value for the conversion factor, C, discussed previously), we matched his reported energy value of −325.1 kJ/mol; however, in those S_6-restricted simulations, our computed distance and angular coordinates differed from those reported by van de Waal. Specifically, our values differed by (+0.05 Å, −0.08 Å) in R, (+0.02, +0.06 Å) in z (distance from the $x-y$ plane), and (−0.53°, +1.02°) in the molecular inclination angle. Regardless of the reasons underlying the discrepancies, our work has identified a lower energy structure for this parameter set.

C. Structures based on the Shi(5) Parameters. The ground-state structure (at 0.01 K) calculated from the Shi(5) parameter set has an energy of −325.096 kJ/mol, and C_i symmetry; the cluster's inversion center coincides with the coordinate system origin. The structure contains six symmetry-distinct pairs of ligand molecules, the coordinates of which are summarized in Table 7. For the equatorial molecules (2, 3, and 4), distances from the cluster center are 5.459, 4.956, and 5.067 Å; distances from the $x-y$ plane are 2.433, 0.159, and 0.309 Å; angles of inclination are 69.19°, 89.38°, and 87.25°, and stabilization energies are −21.49, −23.19, and −24.61 kJ/mol, respectively. For the cap molecules (8, 9, and 10), distances from the cluster center are 5.326, 5.465, and 5.194 Å; distances from the $x-y$ plane are 4.604, 3.256, and 4.671 Å; angles of inclination are 74.71°, 42.20°, and 90.38°, and stabilization energies are −22.89, −22.48, and −24.20 kJ/mol. The central molecule's stabilization energy is −47.390 kJ/mol. Our computed ground-

TABLE 7: Molecular Coordinates for the Ground-State Structure (0.01 K), Based on the Shi(5) Parameter Set (E = −325.10 kJ mol^{-1})[a]

molecule	E (0.11)	R (0.017)	Θ (0.005)	Φ (0.012)	α (0.024)	β (0.015)	γ (0.019)
2	−21.492	5.4593	1.1089	1.2358	0.4521	1.2076	2.1997
3	−23.187	4.9564	1.6029	2.2925	4.3255	1.5600	5.7114
4	−24.611	5.0672	1.5099	3.4581	0.8941	1.5229	3.8718
8	−22.889	5.3264	0.5267	6.1654	0.5424	1.3039	2.7901
9	−22.480	5.4646	2.2090	1.1891	4.6990	0.7365	5.8412
10	−24.201	5.1941	0.4525	2.8052	0.7315	1.5774	4.6994

[a] Molecular interaction energies are shown in the second column. Coordinates of the remaining six ligand molecules are generated by sequential application of the C_i symmetry operation. Standard deviations indicated in the first row are based on 1 K simulations with unrestricted symmetry.

TABLE 8: Molecular Coordinates of the Ground-State C_3 Structure (0.01 K), Based on the Shi(3) Parameter Set (E = −326.22 kJ mol^{-1})[a]

molecule	E (0.10)	R (0.018)	Θ (0.006)	Φ (0.009)	α (0.011)	β (0.014)	γ (0.016)
2	−20.914	5.3415	1.3271	1.2996	0.7092	1.3500	1.9751
3	−23.333	4.9522	1.7504	2.3700	4.0904	1.3292	5.8771
8	−24.884	5.3350	0.5660	0.2963	0.7702	1.3038	2.5970
9	−23.793	5.3185	2.5768	1.2943	3.9113	1.3238	0.4618

[a] Standard deviations are derived from symmetry-unrestricted simulations at 1 K.

state structure is in general agreement with details published by Dulles and Bartell;[12] the primary differences are two: our structure is slightly improved in energy (by 0.1 kJ/mol), and it is characterized by C_i symmetry.

The mean coordinate values derived from symmetry-unrestricted simulations at 1 K are in good agreement with the ground-state coordinates in Table 7. The energy of the static average configuration is −325.07 kJ/mol, whereas the mean cluster energy at 1 K is −324.5 kJ/mol. Although most of the average coordinates are within ±0.003 of their respective ground-state values, one distance coordinate, R(4), differs by −0.012 Å; the maximum angular coordinate deviation from the ground state, −0.034, is observed in Euler coordinate, γ(9). All average molecular interaction energies agree with ground-state values within 0.01 kJ/mol. Composite standard deviations of the average coordinates in the 1 K simulations are included in the first row of Table 7.

D. Structures based on the Shi(3) Parameters. The ground-state cluster calculated from the Shi(3) parameters has C_3 symmetry and an energy of −326.222 kJ/mol. Coordinates of four symmetry-distinct ligand molecules (2, 3, 8, and 9) are collected in Table 8. The upper equatorial molecules are located at a distance of 5.342 Å from the cluster center, 1.289 Å from the $x-y$ plane, and are inclined at an angle of 77.35°; their lower equatorial counterparts are located at R = 4.952 Å, 0.885 Å from the $x-y$ plane, with an inclination angle of 76.16°. The upper cap molecules are located at R = 5.335 Å, 4.503 Å from the $x-y$ plane, with an inclination angle of 74.70°; the lower cap has a distance of 5.513 Å, is located 4.493 Å from the $x-y$ plane, and is characterized by an inclination of 75.85°. The stabilization of the central molecule in this structure is −47.442 kJ/mol; stabilization energies of the ligand molecules are summarized in Table 8. The center of mass of the ligand molecules is located at z = +0.1035 Å.

The mean cluster energy in symmetry-unrestricted simulations at 1 K is −326.0 kJ/mol, whereas the energy of the static average structure is −326.21 kJ/mol; all average coordinate values are in agreement (±0.006) with the ground-state C_3 structure. The average molecular stabilization energies agree with those of the ground state within ±0.1 kJ/mol. Standard deviations of the average coordinates in the simulations at 1 K are included in Table 8.

TABLE 9: Molecular Coordinates of the C_3 Ground-State Structure (0.01 K), Based on the Karlström Parameter Set (E = −372.96 kJ mol^{-1})[a]

molecule	E (0.10)	R (0.018)	Θ (0.013)	Φ (0.018)	α (0.016)	β (0.017)	γ (0.016)
2	−24.372	5.1894	1.3376	1.2762	0.6993	1.2868	1.9928
3	−27.087	4.7365	1.7444	2.3580	4.1160	1.3180	5.8526
8	−28.015	5.1585	0.5661	0.2714	0.7698	1.3076	2.5683
9	−26.852	5.1398	2.5716	1.2915	3.9139	1.3187	0.4426

[a] Standard deviations are derived from simulations at 1 K. The interaction energies and distances must be viewed with skepticism because of scaling issues associated with the parameter set's use with benzene dimers.

E. Structures based on the Karlström Parameters. The 0.01 K ground-state structure determined from the Karlström parameters also has C_3 symmetry and a calculated energy of −372.960 kJ/mol. Coordinates of four symmetry-distinct ligand molecules (2, 3, 8, and 9) are collected in Table 9. The upper equatorial molecules are located at a distance of 5.189 Å from the cluster center, 1.199 Å from the $x-y$ plane, and are inclined at an angle of 73.73°; their lower equatorial counterparts are located at R = 4.737 Å, 0.818 Å from the $x-y$ plane, with an inclination of 75.51°. The upper cap molecules are found at R = 5.158 Å, 4.354 Å from the $x-y$ plane, with an inclination angle of 74.92°; the lower cap ligands are at R = 5.140 Å, are located 4.327 Å from the $x-y$ plane, and have an inclination of 75.56°. The stabilization of the central molecule in this structure is −53.970 kJ/mol; stabilization energies of the ligand molecules are summarized in Table 9. In this C_3 structure, the center of mass of the ligand molecules is located at z = + 0.102 Å.

The energy of the static average (C_3) structure at 1 K is −372.91 kJ/mol, and the mean cluster energy in the symmetry-unrestricted simulations is −372.4 kJ/mol. Average coordinate values are in agreement with the ground-state C_3 structure, differing by no more than ±0.004; average molecular stabilization energies agree with ground-state values to the first decimal. Standard deviations of the average coordinates (in 1 K simulations) are included in Table 9.

It must be noted that both energy and distance scaling problems have been identified when the parameter set is applied to benzene dimers.[15] As a result, these energy values and distance coordinates must be viewed with caution. We have included all of the *angular* coordinates in our statistical analysis, but we have consistently omitted both the energy and distance values.

F. Structures based on the Easter(B13) Parameters. The 0.01 K ground-state structure determined from the Easter(B13) parameters has C_i symmetry and an energy of −325.116 kJ/mol. The structure contains six symmetry-distinct pairs of ligand molecules, the coordinates of which are summarized in Table 10. For the equatorial molecules (2, 3, and 4), distances from the cluster center are 5.506, 5.146, and 5.242 Å; distances from the $x-y$ plane are 1.638, 0.959, and 0.530 Å; angles of inclination are 77.45°, 75.22°, and 83.12°, and stabilization energies are −21.94, −22.96, and −23.55 kJ/mol, respectively. For the cap molecules (8, 9, and 10), distances from the cluster center are 5.401, 5.498, and 5.469 Å; distances from the $x-y$ plane are 4.743, 4.038, and 4.585 Å; angles of inclination are 78.00°, 48.66°, and 81.75°, and stabilization energies are −23.61, −23.48, and −23.81 kJ/mol. The central molecule's stabilization energy is −46.44 kJ/mol.

TABLE 10: Molecular Coordinates for the Ground-State C_i Structure (0.01 K), Based on the Easter(B13) Parameter Set ($E = -325.12$ kJ mol^{-1})[a]

molecule	E (0.11)	*R* (0.017)	Θ (0.005)	Φ (0.012)	α (0.024)	*β* (0.015)	*γ* (0.019)
2	−21.935	5.5060	1.2687	1.3137	0.6022	1.3517	2.0294
3	−22.960	5.1456	1.7582	2.3379	4.0758	1.3129	5.8513
4	−23.547	5.2425	1.4696	3.4464	0.9625	1.4507	3.8861
8	−23.607	5.4013	0.4989	0.2372	0.6832	1.3613	2.6826
9	−23.478	5.4981	2.3957	1.1645	4.1690	0.8493	0.1252
10	−23.809	5.4690	0.5767	2.5549	0.8387	1.4268	4.7393

[a] Molecular interaction energies are shown in the second column. Standard deviations indicated in the first row are based on 1 K simulations with unrestricted symmetry.

The mean coordinate values derived from symmetry-unrestricted simulations at 1 K are in agreement with the ground-state coordinates in Table 10. The energy of the static average configuration is −325.06 kJ/mol, whereas the mean cluster energy at 1 K is −324.8 kJ/mol. All average molecular interaction energies agree with ground-state values within 0.07 kJ/mol. Composite standard deviations of the average coordinates are included in the first row of Table 10.

During the process of deriving the Easter(B13) parameter set, it was observed that when the potential's electrostatic term is weighted more heavily relative to the other four terms, the C_3 structure becomes favored. In our simulations, a C_3 structure, only 0.224 kJ/mol higher in energy than the C_i structure, was observed. In simulations at 1 K with the C_3 structure as the initial configuration, the cluster was *not* transformed to the lower-energy C_i structure over 10^6 Monte Carlo steps. This outcome suggests the possibility that two isomers (C_3 and C_i) may be separated by a kinetic barrier that is sufficient to retard their interconversion at low temperature. (Note, however, that the C_3 structure does *not* correspond to a local energy minimum in this parameter set; subsequent cooling to 0.01 K ultimately effects transformation from the C_3 to the C_i structure.)

V. Discussion and Analysis

A. Symmetries of Theoretical Structures. The simulations described above have resulted in the optimization of all three previously published $(C_6H_6)_{13}$ structures; furthermore, the symmetries of the three structures have been identified. The six computed ground-state structures (0.01 K) differ in their specific details. The Williams parameters forecast the highest symmetry (S_6), the Shi(5) and Easter(B13) parameters predict the lowest (C_i), and the remaining parameter sets predict C_3 symmetry. When *average* molecular coordinates are evaluated from simulations at 1 K, the average structural symmetry from the Williams parameters is *lowered* to C_3; each of the other averaged structures reflects the symmetry of its ground state. Thus, four *averaged* structures (1 K) are C_3, and two are C_i.

It is interesting to observe that symmetries predicted by the four *derived* parameter sets are lower than symmetry predictions of the *parent* parameters. The van de Waal and Shi(3) parameter sets, derived from the Williams parameters, both predict a C_3 structure, whereas the Williams parameters predict S_6. Similarly, the Shi(5) and Easter(B13) parameter sets predict a lower symmetry (C_i), compared to their parent (Karlström), which forecasts C_3.

B. Dependence of Symmetry on the Functional Form of the Parameter Set. Development of the Shi(5) parameter set was motivated by the desire to facilitate rapid computation.[15] Among other modifications, the electrostatic term of the Karlström parameter set was replaced by a parametrized sum, involving a quadratic term and a constant. As observed by Shi, the validity of substituting the true electrostatic term with a term of the form $Dr^{-2} + K$ relies "on the assumption that the most important role of electrostatic interactions is that expressing the short-range preferences of hydrogens and carbons to associate with each other while avoiding contacts with like atoms. It is supposed that the long-range Coulomb effects are unimportant because of extensive cancellations and dielectric polarization."[15] Because the structure calculated from the Shi(5) parameter set is disparate from that of its parent (Karlström), and is also at odds with three of the other parameter sets employed in this study, it seemed advisable to look at the parameter-dependence of the computational results.

Supplemental simulations were conducted to explore the effect of modifying the electrostatic term in several of the potential energy functions. When the electrostatic term was completely omitted, both the Shi(3) and van de Waal structures lost all symmetry; however, the resulting Williams structure retained its S_6 symmetry (although all molecular coordinates were modified). However, parametrization of the Shi(3) electrostatic term with a sum (quadratic plus constant) did not affect the final symmetry. Furthermore, replacement of the quasielectrostatic sum in the Shi(5) function with a pure Coulombic term had no affect on the predicted C_i symmetry. The first conclusion drawn from these supplemental simulations is that the C_i symmetry of the Shi(5) structure is *not* an artifact of the choice to parametrize the electrostatic term; this offers support for Shi's assumption that polarization of the medium (i.e., the surrounding molecules) effectively results in the electrostatic interactions falling off faster than the $1/r$ Coulomb dependence.[15] A second conclusion is based on results from benzene dimer simulations: a significant parameter-dependence is observed on predicted structures of the benzene dimer;[15] the differences in preferred dimer benzene−benzene orientations must certainly affect the computed structures of larger clusters. Finally, as observed previously, the weighting of the electrostatic term (relative to the short-range interaction terms) in the potential energy function can have an affect on predicted structural symmetries.

C. Two Distinct Low-Energy Structures. These simulations lead us to the hypothesis that there may be *two* distinct low-energy $(C_6H_6)_{13}$ structures, both of which are represented in molecular beam experiments. Simulations at 1 K using the Easter(B13) parameters suggest a kinetic barrier that effectively retards conversion between the two forms. This hypothesis gains support from the observation that five of the six parameter sets yield distinct low-energy C_3 and C_i structures, even though only one of the two corresponds to the potential energy minimum for any given parameter set. Although the combined simulations do not unambiguously identify which of the two forms is lower in energy, they are consistent in predicting that the C_3 and C_i forms should have energies that differ by ∼0.2 kJ/mol. (The value for Shi(5) is larger, with a predicted difference of ∼2 kJ/mol.) It is proposed that a $(C_6H_6)_{13}$ cluster formed during free jet expansion may solidify into either of the two configurations and that the rate of conversion between configurations is slow relative to the time scale of a molecular beam experiment.

This two-structure hypothesis is based in the supposition that the parameter sets are each *close* but that none is perfect in its description of the true force field. It is therefore reasonable to expect that the truth may be discovered through a synthesis of the results. None of the six parameter sets separately identifies both C_3 and C_i structures as corresponding to distinct (local) potential energy minima. Nevertheless, given that both structures

TABLE 11: Coordinates and Their 95% Confidence Limits (in Brackets) for the Consolidated (Benzene)$_{13}$ Structure in the C_3 Configuration[a]

molecule	R (0.015)	Θ (0.005)	Φ (0.008)	α (0.011)	β (0.013)	γ (0.013)
2	5.38 [0.09]	1.344 [0.013]	1.293 [0.016]	0.740 [0.044]	1.320 [0.039]	1.938 [0.048]
3	5.09 [0.16]	1.752 [0.007]	2.363 [0.010]	4.074 [0.038]	1.327 [0.010]	5.890 [0.043]
8	5.43 [0.10]	0.571 [0.006]	0.275 [0.018]	0.775 [0.010]	1.303 [0.012]	2.574 [0.019]
9	5.42 [0.10]	2.570 [0.008]	1.295 [0.010]	3.918 [0.012]	1.315 [0.013]	0.450 [0.013]

[a] Results from the Williams average structure at 1 K were used; the radial coordinates from the Karlström parameter set were omitted. Standard deviations (first row) measure displacement due to thermal motion at 1 K.

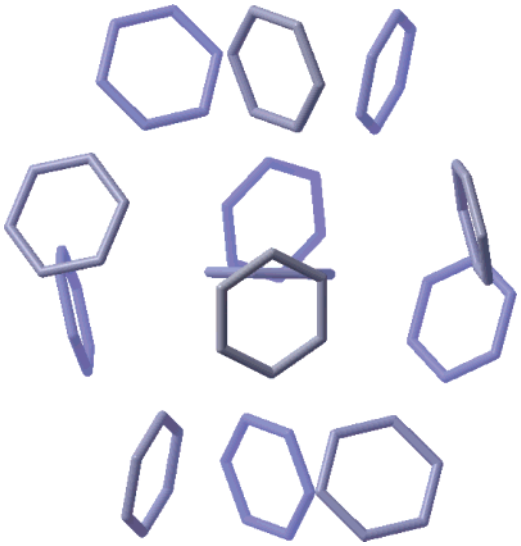

Figure 4. Composite C_3 structure at 1 K, viewed from the $x-y$ plane. Six ligand molecules alternate above (~1.2 Å) and below (~0.9 Å) the plane. The cluster contains an upper cap and a lower cap, with each cap consisting of three molecules. The caps are situated ~4.6 Å from the plane. The sharper, darker hexagons represent benzene molecules closer to the viewer.

have nearly equivalent energies within each parameter set, and that the identity of the lower energy structure varies among the parameter sets, it is reasonable to suppose that the true force field may result in both structures having nearly equal energies, with both corresponding to distinct local minima on the potential energy surface. Although the hypothesis is not proved through the simulations, it gains substantial support from experimental results (below). In keeping with the two-structure hypothesis, we have determined *composite* cluster structures for both isomers.

1. Composite C_3 Structure. The molecular coordinates and their 95% confidence limits for the C_3 composite structure are shown in Table 11. Averages are determined from the optimized C_3 structures of six parameter sets. In this analysis, the ground-state Williams S_6 structure was replaced with the averaged Williams C_3 structure (1 K); because of scaling issues, distance coordinates of the Karlström structure were disregarded. 95% confidence limits are determined by Student t distribution analysis and relate to *mean* coordinate *values*; the composite standard deviations of each molecular coordinate about its mean (from thermal motion at 1 K) are included in the first row of Table 11.

The C_3 $(C_6H_6)_{13}$ structure defined by the coordinates in Table 11 is illustrated in both Figure 4 and Figure 5. Figure 4 views the cluster from the $x-y$ plane, whereas Figure 5 presents a view from the z axis. The upper cap, upper equatorial, lower equatorial, and lower cap molecules can be distinguished in Figure 4, whereas the cluster's 3-fold rotational symmetry is enhanced in Figure 5. The energy of the composite C_3 structure, computed separately from the five parameter sets (Karlström excluded), averages −319.9 ± 3.0 kJ/mol, corresponding to 98.3% of the average optimal configuration energy (−325.4 ± 0.5 kJ/mol). The composite structure plainly occupies a region near the energy minimum for each of the five parameter sets.

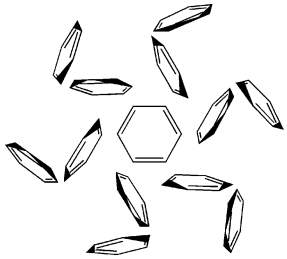

Figure 5. Composite C_3 $(C_6H_6)_{13}$ structure at 1 K, viewed from the z axis. The 3-fold rotational axis is enhanced in this perspective. Molecules that *appear* to be closer to the central molecule represent the upper and lower cap molecules ($R \approx 5.4$ Å); molecules that *appear* to be further from the cluster center represent the upper and lower equatorial molecules ($R \approx 5.4$ and 5.1 Å).

2. Composite C_i Structure. The molecular coordinates and their 95% confidence limits for the C_i composite structure are shown in Table 12. Averages are determined from the optimized C_i structures of five parameter sets; the Williams structure was not included (because it was not uniquely C_i), and the distance coordinates of the Karlström structure were disregarded.

The C_i $(C_6H_6)_{13}$ structure defined by the coordinates in Table 12 is illustrated in both Figure 6 and Figure 7. Figure 6 views the cluster from the $x-y$ plane, whereas Figure 7 presents a view from the z axis. The energy of the composite C_i structure, computed separately using five parameter sets (Karlström excluded), averages −316.3 ± 4.2 kJ/mol, corresponding to 97.2% of the *average* optimal configuration energy (−325.4 ± 0.5 kJ/mol). A direct comparison of the structures in Figures 4 and 6 reveals that, in comparison to the C_3 structure, one of the equatorial molecule pairs in the C_i structure (molecules 2 and 5) is further from the $x-y$ plane, whereas the other equatorial pairs are both closer to the plane. Furthermore, one of the cap pairs (molecules 9, 12) is ~0.4 Å closer to the $x-y$ plane compared to the other cap molecules. Inversion symmetry is present only in the C_i structure. A direct comparison between Figures 5 and 7 reveals the absence of rotational symmetry within the C_i structure.

As a quantitative comparison between the C_3 and C_i structures, differences between corresponding molecular positions and orientations are presented in Table 13. Distances are given in angstroms, and angles are in degrees. To undergo transformation from the C_3 to the C_i structure, each of the 12 ligand molecules would have to be translated by an average of 0.55 ± 0.17 Å. Molecules 9 and 12 would require the greatest adjustment, both in position (0.7 Å) and in angle of inclination (12°). The tabulated differences confirm that the two structures are distinct. Furthermore, if it is accepted that both structures correspond to distinct local energy minima, the structural

TABLE 12: Coordinates and Their 95% Confidence Limits (in Brackets) for the Consolidated (Benzene)$_{13}$ Structure in the C_i Configuration[a]

molecule	R (0.015)	Θ (0.005)	Φ (0.008)	α (0.011)	β (0.013)	γ (0.013)
2	5.48 [0.11]	1.25 [0.10]	1.27 [0.04]	0.59 [0.11]	1.28 [0.08]	2.06 [0.11]
3	5.07 [0.19]	1.71 [0.08]	2.32 [0.02]	4.14 [0.13]	1.38 [0.13]	5.81 [0.08]
4	5.15 [0.17]	1.44 [0.06]	3.45 [0.01]	0.91 [0.04]	1.42 [0.08]	3.88 [0.01]
8	5.37 [0.13]	0.54 [0.03]	0.14 [0.18]	0.69 [0.11]	1.32 [0.03]	2.65 [0.11]
9	5.48 [0.11]	2.44 [0.18]	1.25 [0.09]	4.14 [0.41]	1.10 [0.35]	0.20 [0.48]
10	5.36 [0.22]	0.53 [0.06]	2.53 [0.21]	0.78 [0.05]	1.41 [0.13]	4.68 [0.05]

[a] Data from the Williams parameter set were omitted, as were radial coordinates from the Karlström parameter set. Standard deviations (first row) are a measure of thermal displacement from mean coordinate positions at 1 K.

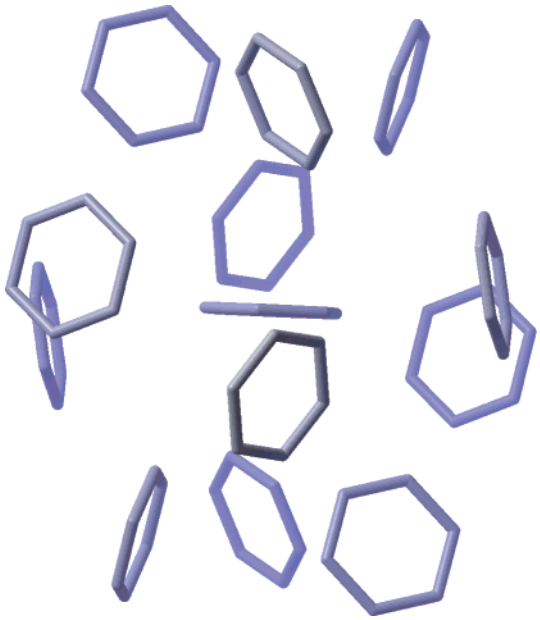

Figure 6. Composite C_i structure at 1 K, viewed from the $x-y$ plane. Six equatorial molecules alternate above and below the plane. The cluster contains an upper cap and a lower cap, each consisting of three molecules.

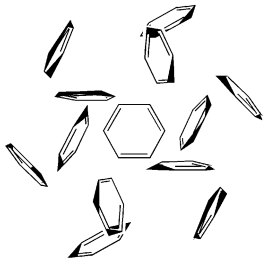

Figure 7. Composite C_i $(C_6H_6)_{13}$ structure at 1 K, viewed from the z axis. The structure has inversion symmetry but lacks a rotational axis.

differences are large enough that interconversion should proceed slowly at low temperatures.

A visual comparison between positions of molecular centers in the two structures is offered in Figure 8. In the C_3 structure, ligands can be divided into four sets, each set containing three molecules. Each triad defines a plane parallel to the plane of the central molecule. Triads in the C_i structures are symmetrically distanced with respect to the cluster center, but the planes defined by the C_i triads are not parallel to the central molecule.

D. Correlation to Experiment. As outlined in the Introduction, experimental results on $(C_6H_6)_{13}$ have held some ambiguity. The apparent absence of absorption from the cluster's central molecule in the $B_{2u} \leftarrow A_{1g}$ 0_0^0 spectrum tentatively supports a C_3 structure;[3] however, the presence of a doublet feature from

TABLE 13: Differences in Composite Coordinate Values ($C_i - C_3$) for the Twelve Ligand Molecules[a]

molecule	ΔX (Å)	ΔY (Å)	ΔZ (Å)	distance (Å)	Δα (°)	$\Delta\beta$ (°)	$\Delta\gamma$ (°)
2	0.08	−0.08	0.53	0.54	−8.4	−2.5	7.1
3	0.14	0.17	0.23	0.32	3.9	3.0	−4.4
4	0.23	−0.28	−0.52	0.63	9.5	5.7	−9.0
5	−0.26	−0.12	−0.82	0.87	−19.4	−2.9	20.6
6	−0.23	0.08	−0.52	0.58	15.0	3.4	−17.9
7	0.04	0.22	0.23	0.32	−1.6	5.3	4.6
8	−0.11	−0.42	0.05	0.44	−4.9	0.8	4.3
9	0.31	0.53	0.36	0.71	12.4	−12.3	−14.2
10	−0.12	−0.48	0.05	0.49	0.3	6.0	0.7
11	0.13	0.34	−0.07	0.37	−5.0	0.1	6.0
12	−0.38	−0.51	−0.37	0.74	12.5	−11.6	−15.9
13	0.18	0.53	−0.06	0.56	0.2	5.3	2.4

[a] Differences in the Cartesian Coordinates and distances between corresponding molecular centers are in Å; differences in the orientation angles are in degrees.

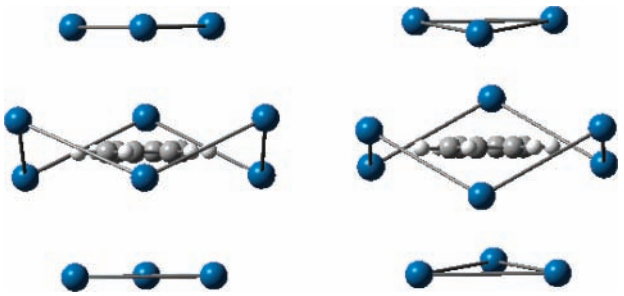

Figure 8. Visual comparison between positions of the ligand molecular *centers* (represented as spheres) in the C_3 (left) and C_i (right) composite structures, viewed from the plane of the central molecule. Lines are added as a viewing aid, separately connecting the upper cap, the (combined) equatorial, and the lower cap ligand positions.

absorption of the central molecule in the isotopically labeled 6_0^1 spectrum argues against the presence of a single cluster structure with C_3 symmetry.[13] The presence of *two* distinct isomers in the cluster beam, separated by less than 1 kJ/mol in energy, could result in a "doublet" feature similar to what is observed in the isotopic labeling experiment.[13] The intensities of the two peaks in the "doublet" are nearly equal, implying that the populations of the two isomers may be approximately equal.

The argument for C_3 symmetry from the $(C_6H_6)_{13}$ 0_0^0 spectrum is based on the *absence* of a specific spectral feature (corresponding to absorption from the central molecule); this absorption is *forbidden* when the central molecule's environment has C_3 (or higher) symmetry.[3] A few comments are in order. First, the feature in question is small (but present) in the 6_0^1 spectrum, where it is *allowed* under C_3 symmetry. Second, the time-of-flight ion signal used to measure the 0_0^0 spectrum is weaker (by two to 3 orders of magnitude) compared to the signal

of the 6_0^1 band. Third, the original hypothesis was based on the assumption that a *single* structural form was present in the cluster beam. Finally, if our hypothesis is correct, that two isomeric forms of the cluster are present in nearly equal concentrations, the absorption in question will be *allowed* for only $\sim 1/2$ of the clusters present. Although the apparent absence of the feature in the 0_0^0 band offers some support, it does not prove the absence of non-C_3 isomers in the cluster beam. If the spectral feature were hypothetically observable, it would be extremely weak; its absence in the 0_0^0 spectrum may simply be a consequence of experimental (signal) limitations. In summary, the proposed presence of two distinct isomers, with C_3 and C_i symmetry, nicely resolves the apparent discrepancy arising from previously published experimental results.

VI. Conclusions

Low-temperature Monte Carlo simulations conducted within a common coordinate system have identified the lowest-energy structure of $(C_6H_6)_{13}$ for each of six distinct potential energy surfaces. The energies reported for previously published structures by Williams,[9] van de Waal,[10] and Bartell[12] were all improved, and the symmetries of the corresponding ground-state structures were identified as S_6, C_3, and C_i, respectively. Symmetries of ground-state structures based on the Shi(3),[15] Karlström,[17] and Easter(B13) potential energy surfaces were determined to be C_3, C_3, and C_i, respectively.

Monte Carlo simulations do not always distinguish between *local* and *global* energy minima. Our work has shown that the three previously published $(C_6H_6)_{13}$ structures, though distinct, all reside within a common, well-localized coordinate space. Although it is conceivable that a distinct and not-yet-identified coordinate region containing the global minimum exists for $(C_6H_6)_{13}$, we deem this unlikely. A remaining difficulty rests in the observation that each potential energy parameter set predicts a cluster structure that, although residing in the common coordinate space, is nevertheless unique in specific structural details. Rather than aiming to identify the "perfect" structure, we have focused in this report on the identification of two *composite* low-energy isomeric structures, each with defined 95% confidence limits; it is proposed that both of these structural forms are present in comparable concentrations under experimental conditions. It is unlikely that more precise structures can be determined until these conclusions have been both tested and confirmed on the basis of experimental data. Easter et al. have measured spectroscopic two-color data for $(C_6H_6)_{13}$ in both the 0_0^0 and 6_0^1 bands of the cluster's $B_{2u} \leftarrow A_{1g}$ vibronic transition.[22] Continuing efforts in our laboratory are focused on interpreting those spectra within a weak-interaction model, with the goal of establishing the precise structure(s) of $(C_6H_6)_{13}$ clusters present in the experimental free jet expansion.

Acknowledgment. The author gratefully acknowledges the Robert A. Welch Foundation (Grant AI-1392) for its generous funding of this work. The author thanks Prof. L. S. Bartell for helpful comments and is grateful for constructive recommendations offered by the Reviewers.

Appendix: Potential Energy Surface Parameters

In section II of this report, the notation of each of the original authors has, in general, been retained. In this Appendix, we describe a system that unifies the notation, and we tabulate parameter values for each of the six potential energy surfaces.

TABLE A1: Potential Energy Parameters for the Six Potential Surfaces Used in This Study[a]

Williams	bond dist	C_{pre}	C_{exp}	C_6	C_1
C−C	1.397	367250	3.60	−2414	32.523
C−H	1.027	65485	3.67	−573	−32.523
H−H		11677	3.74	−136	32.523

van de Waal	bond dist	C_{12}	C_6	C_1
C−C	1.397	4869316	−2765.3	32.523
C−H	1.027	681906	−625.6	−32.523
H−H		89476	−139.4	32.523

Shi(5)	bond dist	C_{12}	C_{10}	C_6	C_2	C_0
C−C	1.401	5930528.0	−2862.0	−1940.9	58.7	−0.407
C−H	1.031	593629.8	−67272.3	184.7	−58.7	0.407
H−H		−32810.2	22886.2	−969.1	58.7	−0.407

Shi(3)	bond dist	C_{12}	C_6	C_1
C−C	1.401	2899300	−2291.0	30.13
C−H	1.031	369090	−433.9	−30.13
H−H		21010	−66.2	30.13

Karlström	bond dist	C_{12}	C_9	C_6	C_4	C_1
C−C	1.395	813034.9	66968.3	−1361.64	−123.294	30.6959
C−H	1.084	115758.7	6868.0	−1199.13	116.688	−30.6959
H−H		13052.8	−2468.6	480.03	−110.081	30.6959

Easter(B13)	bond dist	C_{12}	C_9	C_6	C_4	C_1
C−C	1.395	2315968.0	140670.0	−2109.14	−155.880	25.8549
C−H	1.084	329744.1	14426.6	−1857.42	147.528	−25.8549
H−H		37181.5	−5185.4	743.55	−139.175	25.8549

[a] Distances are in angstroms, and energies are in kJ/mol. Coefficients correspond to the potential energy functional form identified in the text of the Appendix.

In general, atom−atom pair potential energy functions can be expressed in the form

$$V_{ij}(r) = C_{pre}e^{-C_{exp}r_{ij}} + \sum_{n=12}^{0} C_n r_{ij}^{-n}$$

where r_{ij} is the distance between atoms i and j, C_{pre} is the preexponential parameter, C_{exp} is the parameter in the exponential argument, n (which decreases from 12 to zero) is the absolute value of the exponent of r_{ij} in the sum, and C_n is the parameter corresponding to the r^{-n} term. Each of the potential energy parameter sets for benzene−benzene interactions contains three such functions: the first for carbon−carbon interactions, the second for carbon−hydrogen interactions, and the third for hydrogen−hydrogen interactions. Parameter values consistent with this functional form for the six potential energy surfaces considered in this study are collected in Table A1. In all cases, tabulated values are chosen such that the potential energy is in kJ/mol when interaction distances are in angstroms. For the sake of completeness, the fixed carbon−carbon and carbon−hydrogen molecular bond distances (in angstroms) are also tabulated.

References and Notes

(1) Hoare, M. R. *Adv. Chem. Phys.* **1979**, *40*, 49.
(2) Farges, J.; Feraudy, M. F.; Torchet. G. *Adv. Chem. Phys.* **1988**, *70*, 45.
(3) Easter, D. C.; Whetten, R. L.; Wessel, J. E. *J. Chem. Phys.* **1991**, *94*, 3347.

(4) Iimori, T.; Ohshima, Y. *J. Chem. Phys*. **2001**, *114*, 2867.
(5) Börnsen, K. O.; Lin, S. H.; Selzle, H. L.; Schlag, E. W. *J. Chem. Phys*. **1989**, *90*, 1299.
(6) Iimori, T.; Aoki, Y.; Ohshima, Y. *J. Chem. Phys*. **2002**, *117*, 3675.
(7) Iimori, T.; Ohshima, Y. *J. Chem. Phys*. **2002**, *117*, 3656.
(8) Wessel, J. E.; Syage, J. A. *J. Phys. Chem*. **1990**, *94*, 5113.
(9) Williams, D. E. *Acta Crystallogr*. **1980**, *A36*, 715.
(10) van de Waal, B. W. *J. Chem. Phys*. **1983**, *79*, 3948.
(11) van de Waal, B. W. *Chem. Phys. Lett*. **1986**, *123*, 69.
(12) Dulles, F. J.; Bartell, L. S. *J. Phys. Chem*. **1995**, *99*, 17100.
(13) Easter, D. C.; Khoury, J. T.; Whetten, R. L. *J. Chem. Phys*. **1992**, *97*, 1675.
(14) Williams, D. E.; Starr, T. L. *Comput. Chem*. **1977**, *1*, 173.
(15) Shi, X.; Bartell, L. S. *J. Phys. Chem*. **1988**, *92*, 5667.
(16) http://physics.nist.gov/cuu/Constants/index.html. Currently accepted values (1998) are $e = 1.602176462\ (63) \times 10^{-19}$ C.; $N_A = 6.02214199\ (47) \times 10^{23}$ mol^{-1}; $\epsilon_o = 8.854187817 \times 10^{-12}$ F m^{-1}.
(17) Karlström, G.; Linse, P.; Wallqvist, A.; Jönsson, B. *J. Am. Chem. Soc*. **1983**, *105*, 3777.
(18) Niesse, J. A.; Mayne, H. R. *J. Phys. Chem. B* **1997**, *101*, 9137.
(19) Linse, P. *J. Am. Chem. Soc*. **1984**, *106*, 5425.
(20) Frenkel, D.; Smit, B. *Understanding Molecular Simulation: From Algorithms to Applications*. Academic Press: New York, 1996; p 23.
(21) Arfken, G. B.; Weber, H. J. *Mathematical Methods for Physicists*, 4th ed.; Academic Press: New York, 1995; p 188.
(22) Easter, D. C.; Li, X.; Whetten, R. L. *J. Chem. Phys*. **1991**, *95*, 6362.